International Journal of Nanomedicine

Dovepress
open access to scientific and medical research

Open Access Full Text Article

ORIGINAL RESEARCH

Stimulated phase-shift acoustic nanodroplets enhance vancomycin efficacy against methicillin-resistant *Staphylococcus aureus* biofilms

This article was published in the following Dove Press journal:
International Journal of Nanomedicine
30 June 2017
Number of times this article has been viewed

Hao Guo[1]
Ziming Wang[1]
Quanyin Du[1]
Pan Li[2]
Zhigang Wang[2]
Aimin Wang[1]

[1]Department of Orthopedics, Institute of Surgery Research, Daping Hospital, Third Military Medical University, Chongqing, China; [2]Chongqing Key Laboratory of Ultrasound Molecular Imaging, Institute of Ultrasound Imaging, Second Affiliated Hospital of Chongqing Medical University, Chongqing, China

Purpose: Bacterial biofilms on the surface of prostheses are becoming a rising concern in managing prosthetic joint infections. The inherent resistant features of biofilms render traditional antimicrobial therapy unproductive and revision surgery outcomes uncertain. This situation has prompted the exploration of novel antimicrobial strategies. The synergy of ultrasound microbubbles and vancomycin has been proposed as an efficient alternative for biofilm eradication. The purpose of this study was to evaluate the anti-biofilm effect of stimulated phase-shift acoustic nanodroplets (NDs) combined with vancomycin.

Materials and methods: We fabricated lipid phase-shift NDs with a core of liquid perfluoropentane. A new phase change mode for NDs incorporating an initial unfocused low-intensity pulsed ultrasound for 5 minutes and a subsequent incubation at 37°C into a 24-hour duration was developed. Methicillin-resistant *Staphylococcus aureus* (MRSA) biofilms were incubated with vancomycin and NDs under the hybrid stimulation. Biofilm morphology following treatment was determined using confocal laser scanning microscopy and scanning electron microscopy. Resazurin assay was used to quantify bactericidal efficacy against MRSA biofilm bacteria.

Results: NDs treated sequentially with ultrasound and heating at 37°C achieved gradual and substantial ND vaporization and cavitation in a successive process. NDs after stimulation were capable of generating stronger destruction on biofilm structure which was best characterized by residual circular arc margins and more dead bacteria. Furthermore, NDs combined with vancomycin contributed to significantly decreasing the metabolic activity of bacteria in MRSA biofilms ($P<0.05$).

Conclusion: Phase-shift acoustic NDs could exert a significant bactericidal effect against MRSA biofilms through a new stimulation mode. Acoustic NDs present advantages over microbubbles for biofilm damage. This anti-biofilm strategy could be used either alone or as an enhancer of traditional antibiotics in the control of prosthetic joint infections.

Keywords: nanodroplets, MRSA, biofilm matrix, ultrasound, phase change, cavitation

Introduction

Periprosthetic joint infection (PJI) following arthroplasty presents notably morbid consequences to the health of patients, although PJI occurs only in 2.0% and 2.4% of total hip arthroplasties (THA) and total knee arthroplasties (TKA), respectively.[1] As total joint arthroplasties are widely used, the number of PJI is constantly increasing. These infections may render patients extremely agonizing and often require orthopedic surgeons to surgically remove the compromised implant, replace it, and fight the infection with long-term antibiotics, which is costly, demanding but may be unproductive.[2,3] Due to increasing evidence of past decades, bacterial biofilms formed on the surface

Correspondence: Aimin Wang
Department of Orthopedics, Institute of Surgery Research, Daping Hospital, Third Military Medical University, No 10, Daping Changjiang Branch Road, Yuzhong District, Chongqing 400042, China
Tel +86 23 6875 7936
Email trauma2@163.com

Pan Li
Chongqing Key Laboratory of Ultrasound Molecular Imaging, Institute of Ultrasound Imaging, Second Affiliated Hospital of Chongqing Medical University, No 76, Linjiang Road, Yuzhong District, Chongqing 400010, China
Tel +86 136 3798 0781
Email cqlipan@163.com

of implants appear to be a major player in PJI pathogenesis, which has been taken into consideration for the next iteration of PJI guidelines.[4,5]

Microorganisms sequestered in biofilms are characterized by enhanced resistance against common antimicrobial agents and reduced susceptibility to host immune defenses.[6] Because of the inherent resistant properties, biofilms are extremely difficult to eradicate. Of all the factors related to the recalcitrance of biofilm-associated infection, the key may be attributed to the highly complex and variable structure of biofilm matrix, predominantly produced by organisms themselves, which result in markedly decreased penetration of antibiotics and reduced metabolic activity of biofilm-encased bacteria.[7,8] Therefore, there have been growing research efforts on potential candidate strategies targeting disruption of biofilm structure, especially nonoperative, for the sake of improving the efficacy of antimicrobial chemotherapy.

Acoustic cavitation effects, often triggered by either ultrasound (US) alone or US plus microbubbles (MBs), suggest a promising noninvasive method for biofilm eradication when combining with antimicrobial substances. It has been widely accepted that the collapse of MBs leads to transient cavitation that can create pores in cell membranes or holes in blood vessels.[9] Recent studies have found that the cavitation-induced bactericidal effects against biofilms are based upon the cavitationally enhanced antibiotic activity within biofilms and the restored susceptibility of biofilm-encapsulated cells to antibiotic action.[10–13] These effects are of high relevance to the mechanical destruction of biofilm barriers (ie, extracellular matrix), thereby promoting greater penetration of antibiotics surrounding the biofilms into the sessile bacterial community. In the setting of residual matrix scaffold, dormant cells in the deeper layer may recover metabolic activity.[14] The physical fragmentation of matrix seems closely linked to transient cavitation capable of generating high liquid shear forces, free radicals, and high temperatures through US-triggered collapse of gas bubbles rather than stable cavitation with only oscillation of MBs.[11] This trend is particularly more evident when it comes to the addition of exogenous MBs which can significantly lower the cavitation threshold, allowing transient cavitation to occur easily.[15] However, MBs are subject to gas dissolution or spontaneous collapse;[16] thus, it might restrict the intended efficacy and extensive use or need special preparation. More recently, nanodroplets (NDs), typically composed of a shell and a liquid perfluorocarbon core, have shown great promise as a good substitute for bubbles in clinical sonography. When US or thermal energy increases above a certain threshold, NDs would undergo a phase transition into gaseous bubbles, which is called acoustic droplet vaporization (ADV).[17,18] The ADV-generated bubbles are equally supposed to cause mechanical bioeffects to tissues or cells after cavitation.[19] The original liquid phase of NDs may provide a more stable and long-lived structure with smaller size and longer drug payload than MBs.[20] More studies about ADV were present in tumor therapy, but few studies were focused on the influence of ADV on biofilms. Whether the stimulated NDs would be a new and more formidable enhancer of antimicrobial agents against biofilms and what makes the difference of its mechanism are both unknown.

Staphylococcus aureus is recognized to be one of the most common pathogenic organisms causing PJI.[21] However, there has been few studies, relating to cavitation effect on biofilms, include *S. aureus*.[22] In consequence, the aim of this study was to evaluate the anti-biofilm effect of phase-change NDs toward methicillin-resistant *S. aureus* (MRSA) biofilms in vitro with or without vancomycin which is the classical antibiotic specific to Gram-positive infectious organisms. In addition, the ADV of NDs has been primarily activated by focused US or heating above physiological temperature in previous works, and 37°C is believed to be lower than the ADV threshold. Thus, this paper also developed a new mode of phase transition and cavitation through unfocused low-intensity pulsed US followed by incubation at 37°C.

Materials and methods

Bacterial strains and biofilm cultivation

MRSA strain, MRSA252, utilized for biofilm growth in this study, was obtained from the American Type Culture Collection (ATCC, Manassas, VA, USA). Cells were grown in tryptic soy broth (TSB; Oxoid, Basingstoke, UK) overnight at 37°C with agitation. Then, the overnight cultures were inoculated into fresh TSB medium and grown to an $OD_{450\,nm}$ of 0.5. For biofilm growth, coverslip disks of 13 mm diameter (Thermo Fisher Scientific, Waltham, MA, USA) were aseptically placed into a 24-well plate in advance, and approximately 1.5 mL of TSB-diluted cell cultures were added for each well. Then, the 24-well plate was incubated at 37°C without stirring, and 24 hours later accrued biofilms occurred on the coverslip disks.

Preparation and characterization of particles

In this study, for the fabrication of acoustic lipid phase-change droplets, the phospholipid mixture consisted of 1,2-dipalmitoyl-*sn*-glycero-3-phosphocholine (DPPC)

and 1,2-distearoyl-sn-glycero-3-phosphoethanolamine-*N*-[methoxy(polyethylene glycol)-2000] (DSPE-PEG2000) at a weight ratio of 5:2. These materials were purchased from Corden Pharma (Liestal, Switzerland). The lipid components were added to 5 mL chloroform to dissolve in a 100 mL evaporative flask, followed by evaporation to form a thin lipid film via a rotary evaporator (Shanghai Yarong Biochemistry Instrument, Shanghai, China). For the preparation of aqueous phospholipid solution, 2 mL of phosphate-buffered saline (PBS; HyClone; Thermo Fisher Scientific) was added to dissolve the lipid film and disperse it by brief sonication at room temperature. For droplet fabrication, 200 μL perfluoropentane (PFP; J&K Scientific, Beijing, China) was added to the aqueous phospholipid solution. This process must be manipulated in an ice bath to hinder the evaporation of PFP which has a boiling point of 29°C. Then, the mixed solution was subjected to homogenization in the ice bath for 5 minutes via a sonicator (Sonics & Material, Newtown, CT, USA). To remove free phospholipids and excessive reactants, ND emulsions were centrifuged (3,000 *g* ×1 minute) and resuspended in fresh PBS (pH 7.4).

MBs were synthesized as follows: 5 mg DPPC and 2 mg DSPE-PEG2000 were mixed in 0.5 mL of PBS containing 10% glycerol in a vial. After incubation under intermittent shake at 50°C for 30 minutes, the vial was filled with perfluoropropane gas C_3F_8 (Research Institute of Physical and Chemical Engineering of Nuclear Industry, Tianjin, China) and sealed. Then, the vial was subjected to vigorous shaking for 90 seconds by a dental amalgamator (YJT; Shanghai Medical Apparatus and Instruments, Shanghai, China).

Size distribution and potential of both particles were determined by a laser particle size analyzer system (Zetasizer 3000 HS; Malvern Instruments, Malvern, UK). Both of particle solutions were sterilized by ^{60}Co (Sinotex CX, Shanghai, China) irradiation, and the concentration was adjusted to 1×10^9/mL for both particles using PBS.

US exposure setup

All experiments related to US wave delivering were performed by gene ultrasonic transfer machine (UGT 1025; CQMU, Chongqing, China) with an unfocused ultrasonic transducer which was applied at a frequency of 1.0 MHz. The acoustic intensity was set at 3.0 W/cm^2 with a 50% duty cycle. The duration of US transduction was 5 minutes, followed by an antibiotic exposure. The ultrasonic probe whose size of effective area is just over that of one well in 24-well plate was placed underneath the bottom of a well via coupling gels. Such arrangement would contribute to keep cells in the well from the pollution risk, even though the exact energy the probe transmitted was actually lower than 3.0 W/cm^2 due to the obstruction from polystyrene material of plate bottom.

Phase transition and cavitation of NDs

ND stimulation was performed in 24-well plate by two groups: US alone and US plus incubation at 37°C, which were compared with another two groups without US: incubation at room temperature and 37°C. After the first 5 minutes of US exposure, NDs were immediately placed at 37°C or room temperature for further incubation until 24 hours. The morphological changes of NDs in the four groups at initial state, 5 minutes, and 8, 16, and 24 hours were recorded under a light microscope (Olympus Corporation, Tokyo, Japan).

Antibiotic exposure

Vancomycin (Sigma-Aldrich Co., St Louis, MO, USA), reconstituted in distilled water and filter sterilized, was used in our experiment. We use clinically relevant concentrations of vancomycin at 32 mg/L.[23] Antibiotic exposures lasted for 24 hours altogether.

In vitro biofilm treatment

Biofilm interventions were divided into eight groups as follows: nontreatment (control), vancomycin, US, US + vancomycin, US + MBs, US + MBs + vancomycin, US + NDs, and US + NDs + vancomycin. Before the biofilm treatment, particle solution was diluted in the medium per well (1:9), and the final concentration was 10% (v/v). After that, well plates were left in an incubator at 37°C for 24 hours. Biofilms on the coverslip disks were rinsed gently with 0.9% NaCl solution and were used for observation. The treatment of each group was performed in triplicate.

Live/dead staining and confocal laser scanning microscopy

Biofilms remaining on the coverslip disks were stained with the LIVE/DEAD® Baclight™ Bacterial Viability Kit (Molecular Probes, Eugene, OR, USA) as per the manufacturer's protocol. In the kit, SYTO9 stains viable cells green, while propidium iodide (PI) stains dead cells red. Both dyes were simultaneously diluted at the ratio of 1:1,000 in 0.9% NaCl solution and mixed thoroughly. Biofilms were then stained with the dye mixture and incubated at room temperature in the dark for 15 minutes. After being gently rinsed for removal of the unattached dyes, MRSA biofilms were

observed via confocal laser scanning microscope (CLSM; Carl Zeiss Meditec AG, Jena, Germany). ImageJ software was used to analyze live cell ratio.

Resazurin assay

The resazurin assay was conducted as previously described.[24] Prior to experiment, biofilms were formed on a 96-well plate directly without coverslip. After treatment as mentioned earlier, biofilms in wells were rinsed with PBS by gently pipetting to remove planktonic bacteria, with final well volumes settled in 100 μL TSB. Approximately 10 μL Alamar blue (AB; Yeasen, Shanghai, China) was added to each well, followed by plate shaking and incubation at 37°C for 1 hour at 37°C. Absorbance at 570 and 600 nm was obtained using SpectraMax® Plus 384 Microplate Reader (Molecular Devices LLC, Sunnyvale, CA, USA). Percent reduction of AB was determined by the manufacturer's equation.

Scanning electron microscopy

MRSA biofilm samples were rinsed twice in 0.9% NaCl after treatment and then dehydrated through progressively increasing concentrations of both ethanol and tertiary butyl alcohol. After being coated with gold by a coat sputter, samples were imaged with a field-emission scanning electron microscope (SEM; Carl Zeiss Meditec AG).

Statistical analysis

Statistical analysis was conducted using Graphpad Prism 6. One-way analysis of variance with multi-comparisons by Dunnett's or Tukey's test was used to analyze the treatment effects against biofilms. All comparisons with a $P<0.05$ were considered statistically significant.

Results

Characterization of particles

The physicochemical characteristics of both types of particles are listed in Table 1. Initial NDs and MBs exhibited mean diameters of 309 and 1,463 nm, respectively (Figure 1B and C), and the zeta potentials were −16.0 and −6.38 mV, respectively. MBs were constituted by a gas core stabilized by a layer of phospholipid shells, while NDs incorporated the condensed PFP as a liquid core into lipid shells. Because of the different cores, NDs appeared to sink in the bottom that differed from MBs floating on the top of solution in macroscopic images (Figure 1A).

Table 1 Physicochemical characteristics of particles

Sample name	Zeta potential (mV)	Diameter (nm)	PdI
ND	−16.0±3.6	309±67	0.18±0.09
MB	−6.38±1.30	1,463±69	0.25±0.03

Note: Data represent mean ± SD of three independent experiments.
Abbreviations: MB, microbubble; ND, nanodroplet; PdI, polydispersity index.

Phase change and cavitation of NDs

As shown in Figure 2, the NDs preserved at room temperature and 37°C over 24 hours did not show any marked change in size compared with the initial state. Incubation at 37°C seemed more likely to gather NDs. After low-intensity pulsed US stimulation, a minimal number of bubbles transformed into bubbles at once, but the majority of NDs only became a slightly larger in size, keeping mild morphological changes over the 24-hour incubation at room temperature. Samples treated sequentially with US and at 37°C for 8 hours suggested a gradually expanded diameter and possible amalgamations of NDs. Further incubation at 37°C led to a substantial phase transition to bubbles, and then a continuous coalescence of ND-converted nanobubbles into larger bubbles which presented in foam-like shape large enough for macroscopic observation at 16 hours. Ultimately, most of the coalesced bubbles underwent spontaneous cavitation, which reflected an irreversible and steady progress of ADV and cavitation under 24-hour hybrid stimulation of initial unfocused low-intensity pulsed US for 5 minutes and subsequent incubation at 37°C.

Evaluation of biofilm morphology destruction

The anti-biofilm activity of NDs was confirmed through CLSM and SEM. Three-dimensional CLSM images demonstrated that packed and dense biofilms were observed in the nontreatment groups (Figure 3A). Exposure to vancomycin alone did not result in any profound structural changes in biofilms (Figure 3B). However, loosened structure and many micropores were observed after treatment with US or US + MBs (Figure 3C and D). Biofilms treated with US plus vancomycin with or without MBs also exhibited similar loosened morphology with a small number of dead cells (Figure 3E and F). More noticeable destruction in biofilm structure and dead bacteria occurred as a result of the ADV and cavitation from the US + NDs group (Figure 3G). Furthermore, treatment with US + NDs + vancomycin resulted in more sparse biofilm distribution than any other groups (Figure 3H). In the CLSM images, green fluorescence represented viable cells, whereas red fluorescence represented dead cells. Based upon these data, the percentage of viable cells relative to the total cell counts was measured. As indicated in Figure 3I, exposure to US + NDs achieved significantly more bacteria

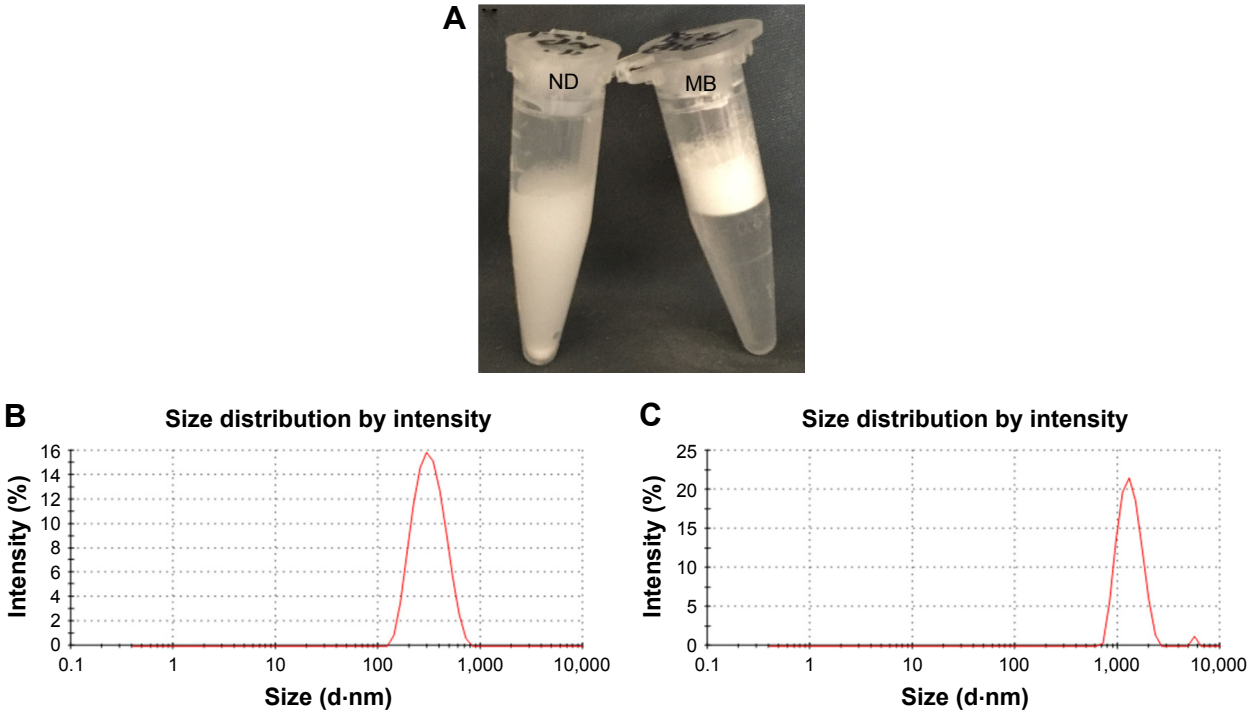

Figure 1 Characterization of ND and MB samples.
Notes: The macroscopic views of ND and MB samples (**A**). The size distribution of ND (**B**) and MB (**C**).
Abbreviations: MB, microbubble; ND, nanodroplet.

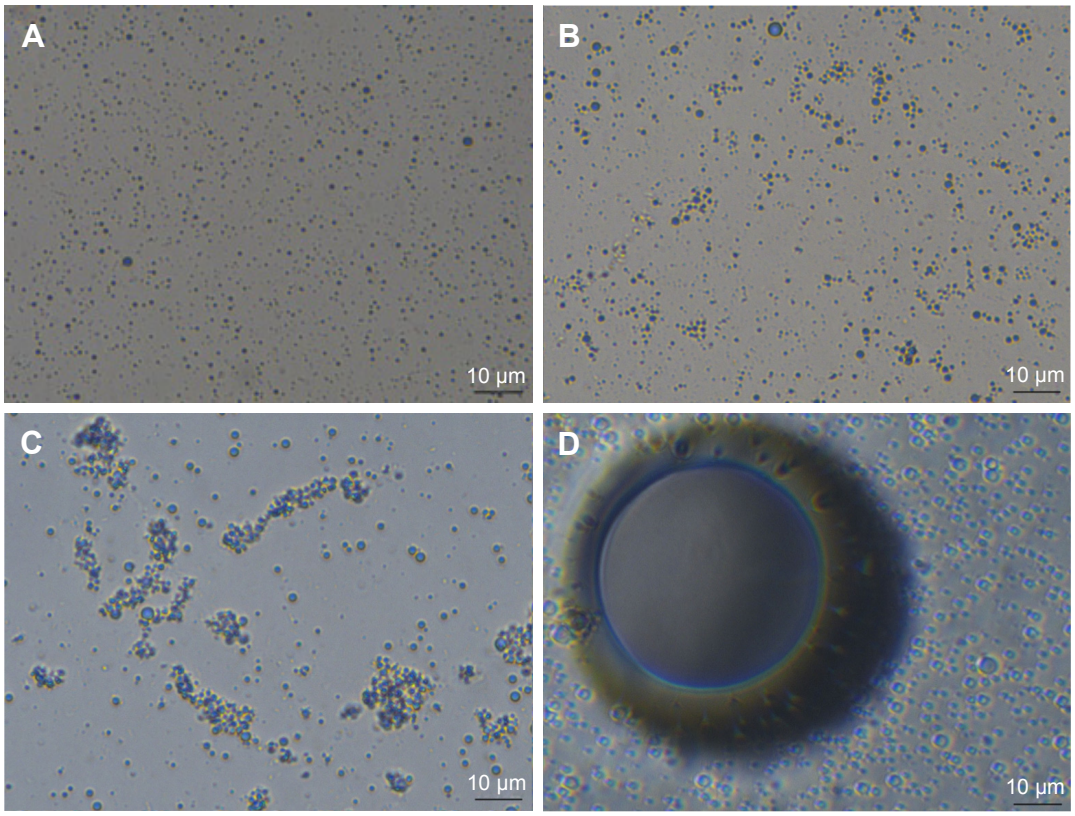

Figure 2 (*Continued*)

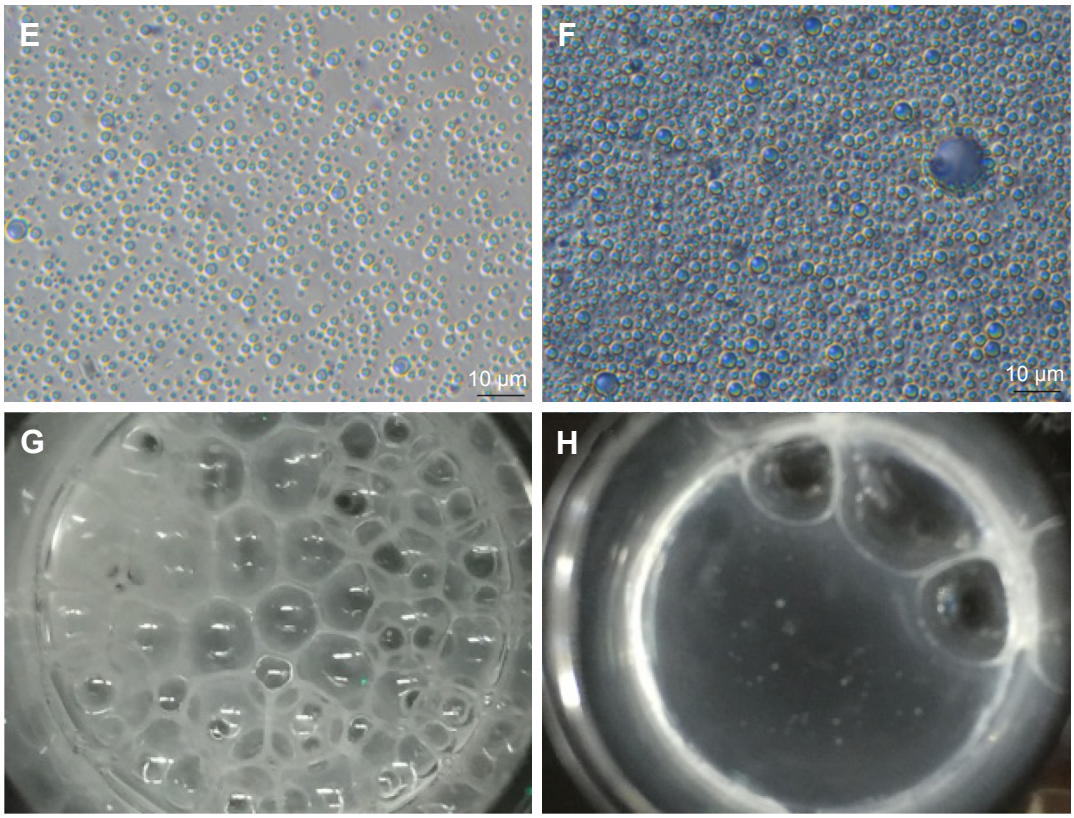

Figure 2 Optical images of NDs.
Notes: Light microscopic images of NDs in initial state (**A**), treated at room temperature for 24 hours (**B**), incubation at 37°C for 24 hours (**C**), US for 5 minutes (**D**), US for 5 minutes and room temperature for 24 hours (**E**), US for 5 minutes and incubation at 37°C for 8 hours (**F**). Macroscopic images of NDs treated with US for 5 minutes and incubation at 37°C for 16 hours (**G**), US for 5 minutes and incubation at 37°C for 24 hours (**H**). Images **A**–**F** are at 400× magnification.
Abbreviations: NDs, nanodroplets; US, ultrasound.

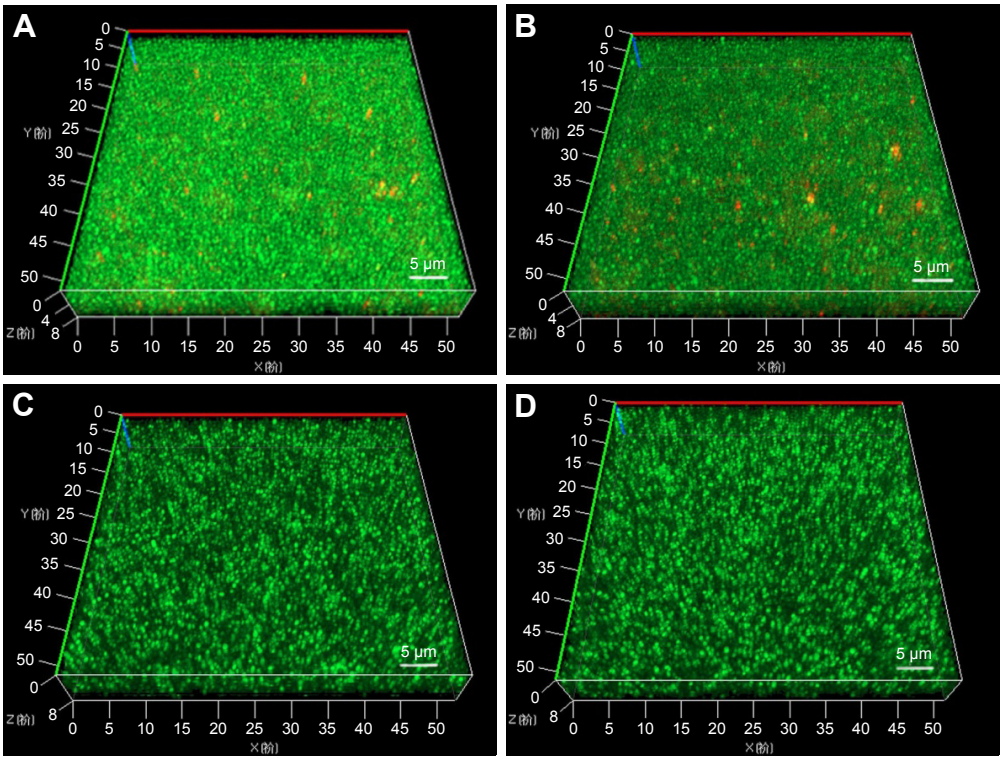

Figure 3 (*Continued*)

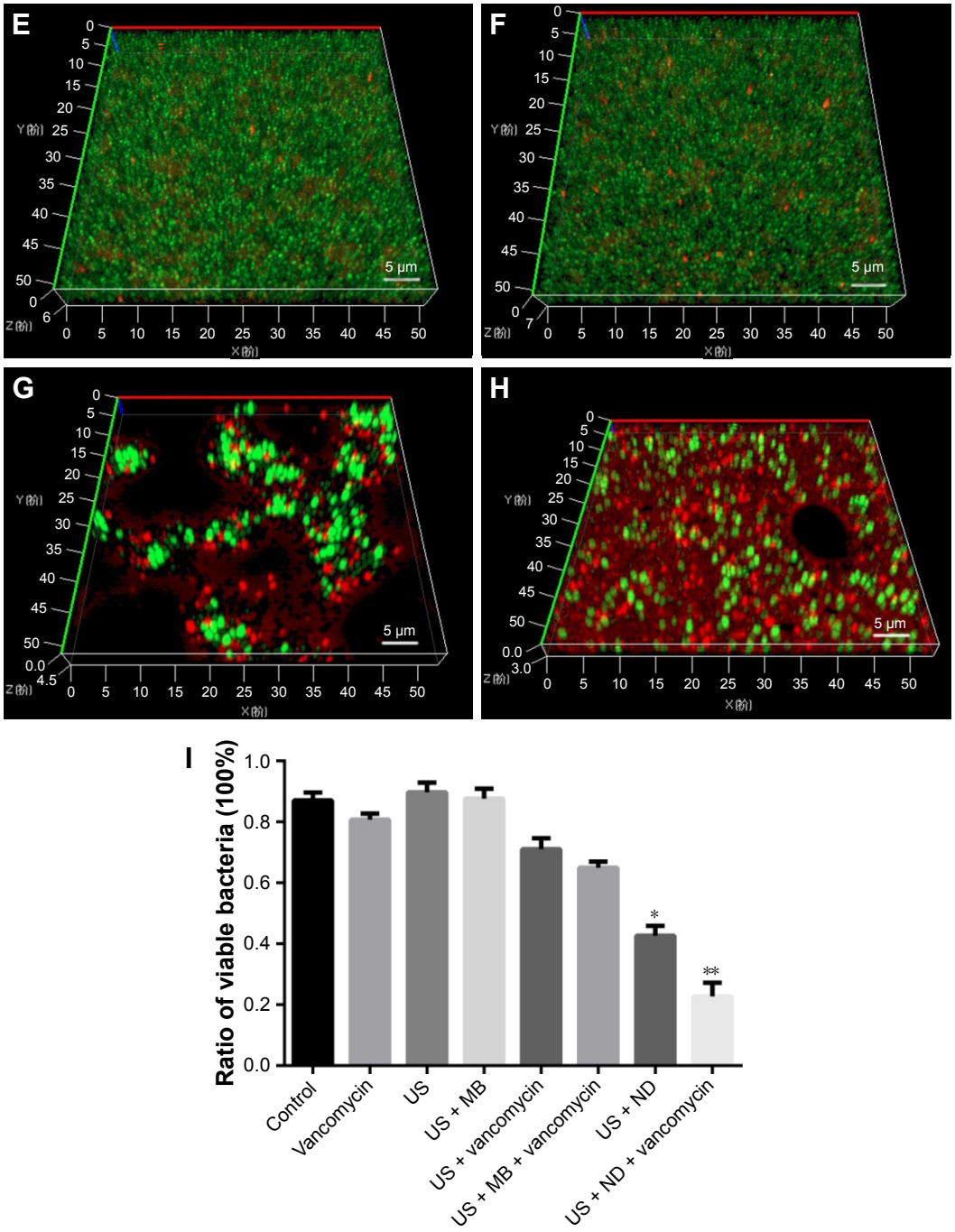

Figure 3 The effect of NDs on MRSA biofilms.

Notes: (**A**–**H**) Three-dimensional CLSM images of MRSA biofilms treated with control (**A**), vancomycin (**B**), US (**C**), US + MBs (**D**), US + vancomycin (**E**), US + MBs + vancomycin (**F**), US + NDs (**G**), and US + NDs + vancomycin (**H**). Then, all groups were incubated at 37°C for 24 hours, followed by live/dead staining. Fluorescent green denotes viable cells, while fluorescent red denotes dead cells. (**I**) Based upon CLSM data, the percentage of viable cells relative to the total cell counts was quantitatively analyzed using ImageJ software. Values represent the mean plus SD of four measurements (*$P<0.05$ compared with other groups excluding US + NDs + vancomycin; **$P<0.01$ compared with all other groups).

Abbreviations: CLSM, confocal laser scanning microscope; MBs, microbubbles; MRSA, methicillin-resistant *Staphylococcus aureus*; NDs, nanodroplets; US, ultrasound.

killing than other treatment, whether vancomycin was present or not. SEM images of MRSA biofilm of partial groups are shown in Figure 4. Control samples appear as typically densely populated bacterial community enclosed in hydrogel matrix, whereas US intervention samples presented partially loosened changes which appeared as formation of dispersed holes in biofilms. In contrast, US + NDs samples presented unique structural changes indicative of NDs-elicited ADV and cavitation damage to biofilms. Large part of biofilms lost adherence to the coverslip disk or each other. A variety of residual circular arc margins, large or small, were observed around biofilm remains, which could be also indicated in

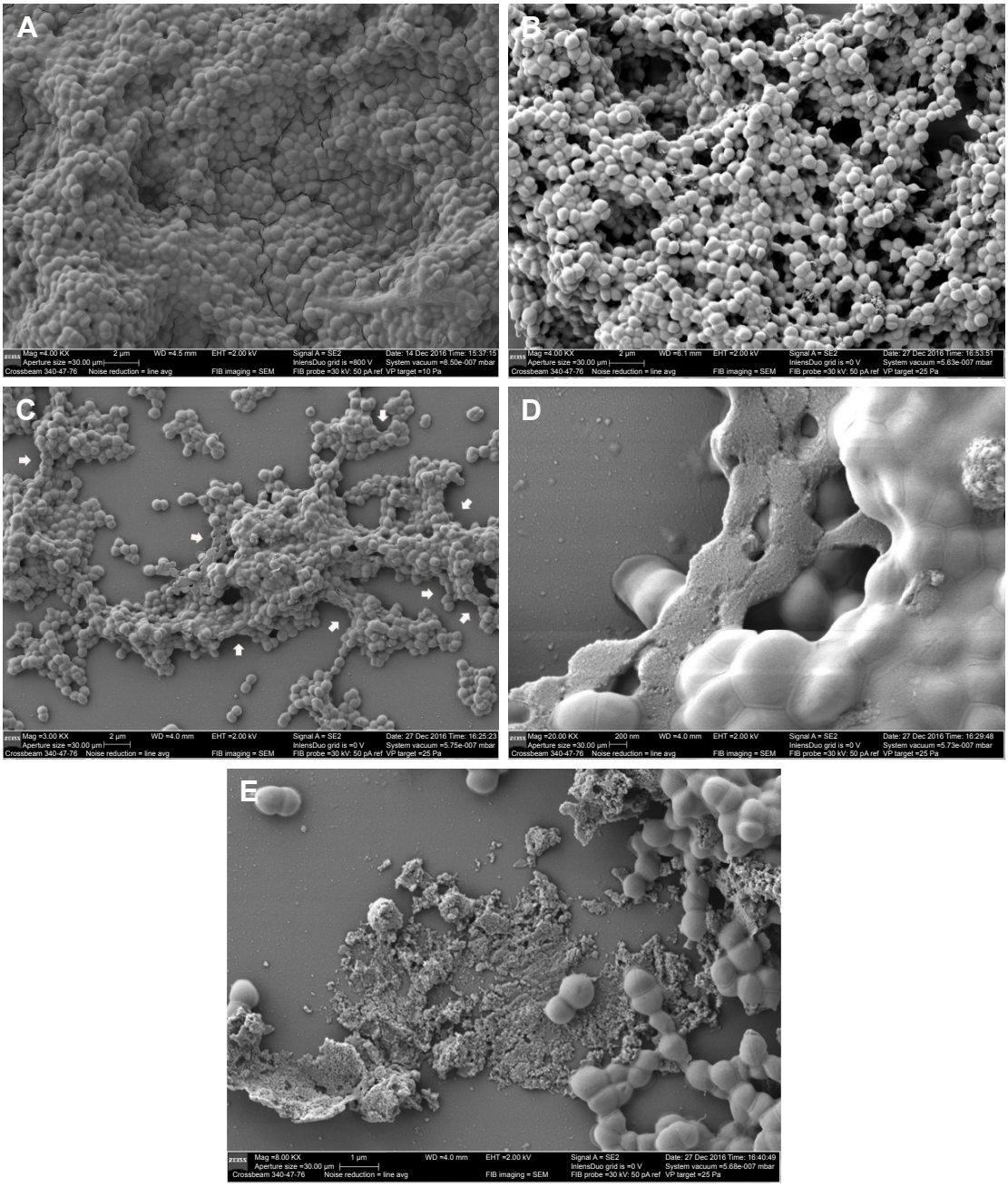

Figure 4 SEM images of MRSA biofilms.
Notes: Biofilms that were exposed to nontreatment (**A**), US (**B**), US + NDs (**C** and **D**), US + NDs + vancomycin (**E**). White arrows in (**C**) present unique structural changes of residual circular arc margins caused by the stimulated NDs, and the image in (**D**) is further observation of the changes at 20,000× magnification.
Abbreviations: MRSA, methicillin-resistant *Staphylococcus aureus*; NDs, nanodroplets; SEM, scanning electron microscope; US, ultrasound.

CLSM images involving NDs (Figure 3G and H). Upon further higher magnification, the damaged bacteria that were located along the circular arc margin became shrunken but remained in cluster arrangement.

Bactericidal efficacy against MRSA biofilm bacteria

CLSM analysis combined with live/dead staining could not fully demonstrate bactericidal effect quantitatively in the single well. Resazurin assay has been suggested to evaluate metabolic cell activity of the entire well in a rapid and reliable way, and *S. aureus* biofilms were reported to be amenable to this viability assay.[24] As shown in Figure 5, the percent reduction of AB in the vancomycin, US, US + vancomycin, US + MBs and US + MBs + vancomycin groups had not any significant difference from that in the control. Application of US or US + MBs in combination with vancomycin saw a significant fall of percent reduction to 31.00%±1.28%

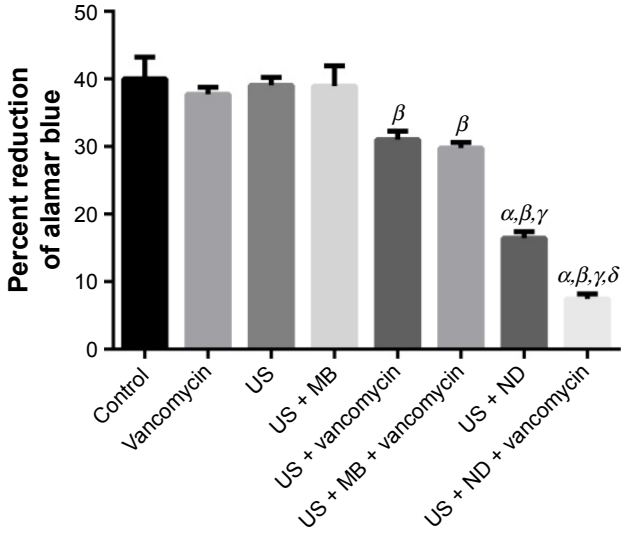

Figure 5 Percent reduction of Alamar blue for MRSA biofilms.
Notes: Data represent mean ± SD of percent reduction of Alamar blue. α indicates $P<0.05$ compared with the control. β indicates $P<0.05$ compared with vancomycin group. γ indicates $P<0.05$ compared with US + MBs + vancomycin treatment. δ indicates $P<0.05$ compared with US + NDs treatment.
Abbreviations: MB, microbubble; MRSA, methicillin-resistant *Staphylococcus aureus*; ND, nanodroplet; US, ultrasound.

and 29.77%±0.83%, respectively, comparing with that in vancomycin-alone treatment (37.73%±1.02%), but they were not significantly different from each other. The most significant decline in percent reduction of AB occurred in the US + NDs group (16.43%±0.95%) and US + NDs + vancomycin group (7.43%±0.76%), comparing with other treatment without NDs. Furthermore, US + NDs + vancomycin treatment exhibited significantly lower percent reduction of AB than US + NDs.

Discussion

Biofilms in periprosthetic infections pose serious challenges to orthopedic surgeons. All the effort underway to combat biofilm infections, whether conservative chemotherapy or surgical management, would not guarantee intended outcomes. Motivated by the enhanced antibiotic effect exerted by acoustic cavitation, the current study is the first to our knowledge to use NDs, a new potential US molecular probe, to investigate a synergistic effect of combining cavitation of NDs and vancomycin against MRSA biofilms in vitro. Our results demonstrated that NDs could significantly enhance bactericidal activity of vancomycin against MRSA biofilms. Particularly, NDs per se showed a potent capability of biofilm bacteria damage under right stimulation, regardless of antibiotics.

To achieve full potential of cavitation bioeffects in NDs, the core of NDs should undergo a phase change first. Although the boiling point of PFP is around 29°C, there is compelling evidence stating that the volatile liquid in droplet forms boils above 37°C due to the surface tension of liquid–liquid interface.[17,25] It could be inferred from this study that physiological temperature alone can hardly inflate the NDs bigger in size, even after heating for 24 hours, which is far from cavitation state. Just relying on the energy from low-intensity pulsed US within the range for clinical use was not powerful enough for substantially eliciting the droplet conversion, which was also verified herein. Instead, researchers prefer high-intensity US, especially focused US, to contribute to effectively vaporizing droplets and allowing them to cavitate.[26–28] However, disadvantages of focused US is evident, such as the safety risk of concomitant thermal damage to normal tissues and poor access to devices. Kripfgans et al[17] previously reported phase transition of PFP droplet in micron size by US within a diagnostic frequency range, but the ADV threshold of smaller droplets might be higher.[29] In this study, the energy accumulation by the sequential treatment incorporating pulsed low acoustic pressure and heating at physiological temperature witnessed a relative less fierce process of ND vaporization and cavitation over 24 hours, which suggests a potential new mode of phase transition and cavitation for nanometer-sized PFP droplets. Although there is not a clear understanding of this process, it is possible that pre-excitation by pulsed low-intensity US may cause a small number of NDs to convert into nanobubbles which may decrease the ADV threshold.[30] Immediately followed by continuous heating at 37°C, preformed nanobubbles may begin to coalesce into larger MBs and the remaining NDs below ADV threshold may start to transcend it to vaporize and then to break up. This mode of vaporization and cavitation may utilize normal physiological temperature as an adjunct for stimulation to offset the energy insufficiency from pulsed low-intensity US. Such mode could be beneficial to further research in vivo and clinical application.

Several studies were carried out to destroy bacteria residing in the biofilms using US-targeted MB destruction.[10,12,13] It has been recognized that MBs can present as cavitation nuclei to lower the cavitation threshold, thereby significantly facilitating transient cavitation which may generate shock waves and microjets.[31] Under such violent physical stress, high-density surfaces (eg, bacterial biofilm) become loose with emerging micropores and craters, allowing antibiotics to penetrate through the weakened matrix barrier and increase antibiotic concentration therein. Arguably, these changes restore the bacterial susceptibility to antibiotics. In the current study, we confirmed again that US could enhance antibiotic activity against biofilms, but US + vancomycin treatment did not show any significant difference from the control. Groups

contained MBs exhibited almost similar results compared to the corresponding groups without MBs (US + MBs vs US and US + MBs + vancomycin vs US + vancomycin). The inactivation of MBs may be attributed to the reason that MBs and NDs differ in core components, with MBs going up to the liquid surface while NDs declining. The resultant long distance between MBs above and biofilms below in the well attenuated the effect of cavitation produced by MBs, so that the previous study kept MBs in close proximity to the biofilms in special apparatus, such as Opticell™ chambers which were enclosed and narrow enough to place MBs and biofilms in only about 2 mm distance, far closer than that between the liquid surface and the biomass at the bottom in our study.[10]

Our results revealed that the activated NDs were powerful enough to cause notable destruction to biofilm structure with some unique characteristics in the process of vaporization and cavitation, and NDs performed better than MBs. We suggest three possible explanations. First, NDs became larger steadily in the continuous and less precipitous process of vaporization and cavitation. The process seemed like inflating a balloon followed by its blasting, adding gradually growing pushing forces to transient cavitation effect against the adjacent biofilms, which means ADV may exert mechanical bioeffects as an independent contributor as reported by Kang et al.[32] Second, numerous constantly expanding converted bubbles may be three to five times larger in diameter than initial sizes, either mutually squeezed the biofilm structure into residues in circular arc shape which were best illustrated in the SEM images or merged into larger bubbles that may release more shock waves and free radicals during collapse. A variety of cavitation events adjacent to biofilms may generate stresses on the tenacious cell wells, causing direct stress-induced cell disorganization or death, which could be indicated by the SEM and CLSM images in groups including NDs. Third, although larger gas bubbles could have a more obvious tendency of floating upward in the reactive system, the expanded diameter, constant bubble bursting, and interactive collision altogether may render gas bubbles more vulnerable to cavitation. Consequently, the NDs-induced effect integrating ADV with cavitation is likely to be more powerful than the transient cavitation caused by MBs which are lack of such a dynamic expanding process by themselves and also located far from the biofilms. Strong as it may seem, NDs' cavitation could not kill all the biofilm bacteria on its own yet. The detached flakes of biofilms occurred during the interaction with the activated NDs promoted closer contact with vancomycin than ever, which could explain that US + NDs + vancomycin treatment induced a stronger antibacterial effect than US + NDs.

It is worthy of note that the difference of surface charge occurred between NDs and MBs. We suppose that it was mainly associated with the difference of preparation methods. NDs were fabricated by rotary evaporation followed by homogenization with PFP, while MBs were synthesized through oscillation with C_3F_8 gas. In addition, PBS in MBs' preparation contained 10% glycerol, which might contribute to the difference as well.

As the NDs-induced effects against biofilms are complex, fully understanding the underlying mechanism and further development of this technology require next step research. First, NDs were placed in wells offering an expandable space in vitro in this study, but how does it work exactly against biofilms in vivo needs to investigate. Second, several studies have been using nanoparticles of different types to penetrate biofilm matrix to induce anti-biofilm effect.[33,34] Hence, further investigation of whether initial NDs could enter the biofilm matrix and what performance the activated NDs within the biofilms could behave after phase transition are also required. Third, several factors have impacts on the activity of NDs' vaporization and cavitation against biofilm bacteria, such as physicochemical characteristics of NDs, the US parameters (acoustic intensity, frequency, duty cycle, duration, etc.), assembling pattern between US and heating (sequence and duration), antibiotic category and concentration, bacterial species, etc. Fourth, it has been believed that the types of bacteria can affect the efficacy of US action;[35] thus, it is very necessary to further verify this anti-biofilm strategy in other bacteria. They are all should be taken into account for optimization in the future study. In addition, extensive use of NDs as carrier systems for gene or drug delivery or conjugation to antibodies specific to target bacteria deserves more studies.

Conclusion

Our results reveal that phase-shift acoustic NDs coupled with vancomycin could exert significant bactericidal efficacy against MRSA biofilms through sequential stimulation which is clinically available by low-intensity pulsed US and heating at 37°C. This study also demonstrates that NDs have ascendancy over MBs in terms of mechanical cavitation bioeffects. In spite of incomplete eradication of biofilm bacteria by activated NDs in the current study, this novel strategy could modify itself by optimizing related parameters or play as an enhancer of traditional antimicrobial chemotherapy to achieve preferable killing of biofilm bacteria.

Acknowledgments

The authors gratefully acknowledge Prof Quanming Zou, Dr Jinyong Zhang and Jiang Gu (Department of Microbiology and Biochemical Pharmacy, College of Pharmacy, Third Military Medical University, Chongqing, China) for their assistance and advice.

Disclosure

The author reports no conflicts of interest in this work.

References

1. Kurtz SM, Lau E, Watson H, Schmier JK, Parvizi J. Economic burden of periprosthetic joint infection in the United States. *J Arthroplasty*. 2012;27(8 suppl):61.e1–65.e1.
2. Shahi A, Parvizi J. Prevention of periprosthetic joint infection. *Arch Bone Jt Surg*. 2015;3(2):72–81.
3. Kapadia BH, Berg RA, Daley JA, Fritz J, Bhave A, Mont MA. Periprosthetic joint infection. *Lancet*. 2016;387(10016):386–394.
4. McConoughey SJ, Howlin R, Granger JF, et al. Biofilms in periprosthetic orthopedic infections. *Future Microbiol*. 2014;9(8):987–1007.
5. Tzeng A, Tzeng TH, Vasdev S, et al. Treating periprosthetic joint infections as biofilms: key diagnosis and management strategies. *Diagn Microbiol Infect Dis*. 2015;81(3):192–200.
6. Stewart PS. Antimicrobial tolerance in biofilms. *Microbiol Spectr*. 2015;3(3).
7. Flemming HC, Wingender J. The biofilm matrix. *Nat Rev Microbiol*. 2010;8(9):623–633.
8. Hoiby N, Bjarnsholt T, Givskov M, Molin S, Ciofu O. Antibiotic resistance of bacterial biofilms. *Int J Antimicrob Agents*. 2010;35(4):322–332.
9. Rapoport N. Phase-shift, stimuli-responsive perfluorocarbon nanodroplets for drug delivery to cancer. *Wiley Interdiscip Rev Nanomed Nanobiotechnol*. 2012;4(5):492–510.
10. Dong Y, Chen S, Wang Z, Peng N, Yu J. Synergy of ultrasound microbubbles and vancomycin against *Staphylococcus epidermidis* biofilm. *J Antimicrob Chemother*. 2013;68(4):816–826.
11. Runyan CM, Carmen JC, Beckstead BL, Nelson JL, Robison RA, Pitt WG. Low-frequency ultrasound increases outer membrane permeability of *Pseudomonas aeruginosa*. *J Gen Appl Microbiol*. 2006;52(5):295–301.
12. He N, Hu J, Liu H, et al. Enhancement of vancomycin activity against biofilms by using ultrasound-targeted microbubble destruction. *Antimicrob Agents Chemother*. 2011;55(11):5331–5337.
13. Ronan E, Edjiu N, Kroukamp O, Wolfaardt G, Karshafian R. USMB-induced synergistic enhancement of aminoglycoside antibiotics in biofilms. *Ultrasonics*. 2016;69:182–190.
14. Carmen JC, Nelson JL, Beckstead BL, et al. Ultrasonic-enhanced gentamicin transport through colony biofilms of *Pseudomonas aeruginosa* and *Escherichia coli*. *J Infect Chemother*. 2004;10(4):193–199.
15. Wang JF, Wang JB, Chen H, et al. Ultrasound-mediated microbubble destruction enhances gene transfection in pancreatic cancer cells. *Adv Ther*. 2008;25(5):412–421.
16. Ferrara KW. Driving delivery vehicles with ultrasound. *Adv Drug Deliv Rev*. 2008;60(10):1097–1102.
17. Kripfgans OD, Fowlkes JB, Miller DL, Eldevik OP, Carson PL. Acoustic droplet vaporization for therapeutic and diagnostic applications. *Ultrasound Med Biol*. 2000;26(7):1177–1189.
18. Rapoport NY, Efros AL, Christensen DA, Kennedy AM, Nam KH. Microbubble generation in phase-shift nanoemulsions used as anticancer drug carriers. *Bubble Sci Eng Technol*. 2009;1(1–2):31–39.
19. Pajek D, Burgess A, Huang Y, Hynynen K. High-intensity focused ultrasound sonothrombolysis: the use of perfluorocarbon droplets to achieve clot lysis at reduced acoustic power. *Ultrasound Med Biol*. 2014;40(9):2151–2161.
20. Reznik N, Williams R, Burns PN. Investigation of vaporized submicron perfluorocarbon droplets as an ultrasound contrast agent. *Ultrasound Med Biol*. 2011;37(8):1271–1279.
21. Osmon DR, Berbari EF, Berendt AR, et al. Diagnosis and management of prosthetic joint infection: clinical practice guidelines by the Infectious Diseases Society of America. *Clin Infect Dis*. 2013;56(1):e1–e25.
22. Erriu M, Blus C, Szmukler-Moncler S, et al. Microbial biofilm modulation by ultrasound: current concepts and controversies. *Ultrason Sonochem*. 2014;21(1):15–22.
23. Liu C, Bayer A, Cosgrove SE, et al. Clinical practice guidelines by the Infectious Diseases Society of America for the treatment of methicillin-resistant *Staphylococcus aureus* infections in adults and children: executive summary. *Clin Infect Dis*. 2011;52(3):285–292.
24. Pettit RK, Weber CA, Pettit GR. Application of a high throughput Alamar blue biofilm susceptibility assay to *Staphylococcus aureus* biofilms. *Ann Clin Microbiol Antimicrob*. 2009;8:28.
25. Giesecke T, Hynynen K. Ultrasound-mediated cavitation thresholds of liquid perfluorocarbon droplets in vitro. *Ultrasound Med Biol*. 2003;29(9):1359–1365.
26. Rapoport N, Gao Z, Kennedy A. Multifunctional nanoparticles for combining ultrasonic tumor imaging and targeted chemotherapy. *J Natl Cancer Inst*. 2007;99(14):1095–1106.
27. Schad KC, Hynynen K. In vitro characterization of perfluorocarbon droplets for focused ultrasound therapy. *Phys Med Biol*. 2010;55(17):4933–4947.
28. Rapoport NY, Kennedy AM, Shea JE, Scaife CL, Nam KH. Controlled and targeted tumor chemotherapy by ultrasound-activated nanoemulsions/microbubbles. *J Control Release*. 2009;138(3):268–276.
29. Kripfgans OD, Fabiilli ML, Carson PL, Fowlkes JB. On the acoustic vaporization of micrometer-sized droplets. *J Acoust Soc Am*. 2004;116(1):272–281.
30. Lo AH, Kripfgans OD, Carson PL, Rothman ED, Fowlkes JB. Acoustic droplet vaporization threshold: effects of pulse duration and contrast agent. *IEEE Trans Ultrason Ferroelectr Freq Control*. 2007;54(5):933–946.
31. Postema M, van Wamel A, Lancee CT, de Jong N. Ultrasound-induced encapsulated microbubble phenomena. *Ultrasound Med Biol*. 2004;30(6):827–840.
32. Kang ST, Huang YL, Yeh CK. Characterization of acoustic droplet vaporization for control of bubble generation under flow conditions. *Ultrasound Med Biol*. 2014;40(3):551–561.
33. Lee JH, Kim YG, Cho MH, Lee J. ZnO nanoparticles inhibit *Pseudomonas aeruginosa* biofilm formation and virulence factor production. *Microbiol Res*. 2014;169(12):888–896.
34. Perez-Diaz MA, Boegli L, James G, et al. Silver nanoparticles with antimicrobial activities against *Streptococcus mutans* and their cytotoxic effect. *Mater Sci Eng C Mater Biol Appl*. 2015;55:360–366.
35. Carmen JC, Roeder BL, Nelson JL, et al. Treatment of biofilm infections on implants with low-frequency ultrasound and antibiotics. *Am J Infect Control*. 2005;33(2):78–82.